Volume 36
Number 8
August 2021
Pages 1585–1784

JAAS

Journal of Analytical Atomic Spectrometry

rsc.li/jaas

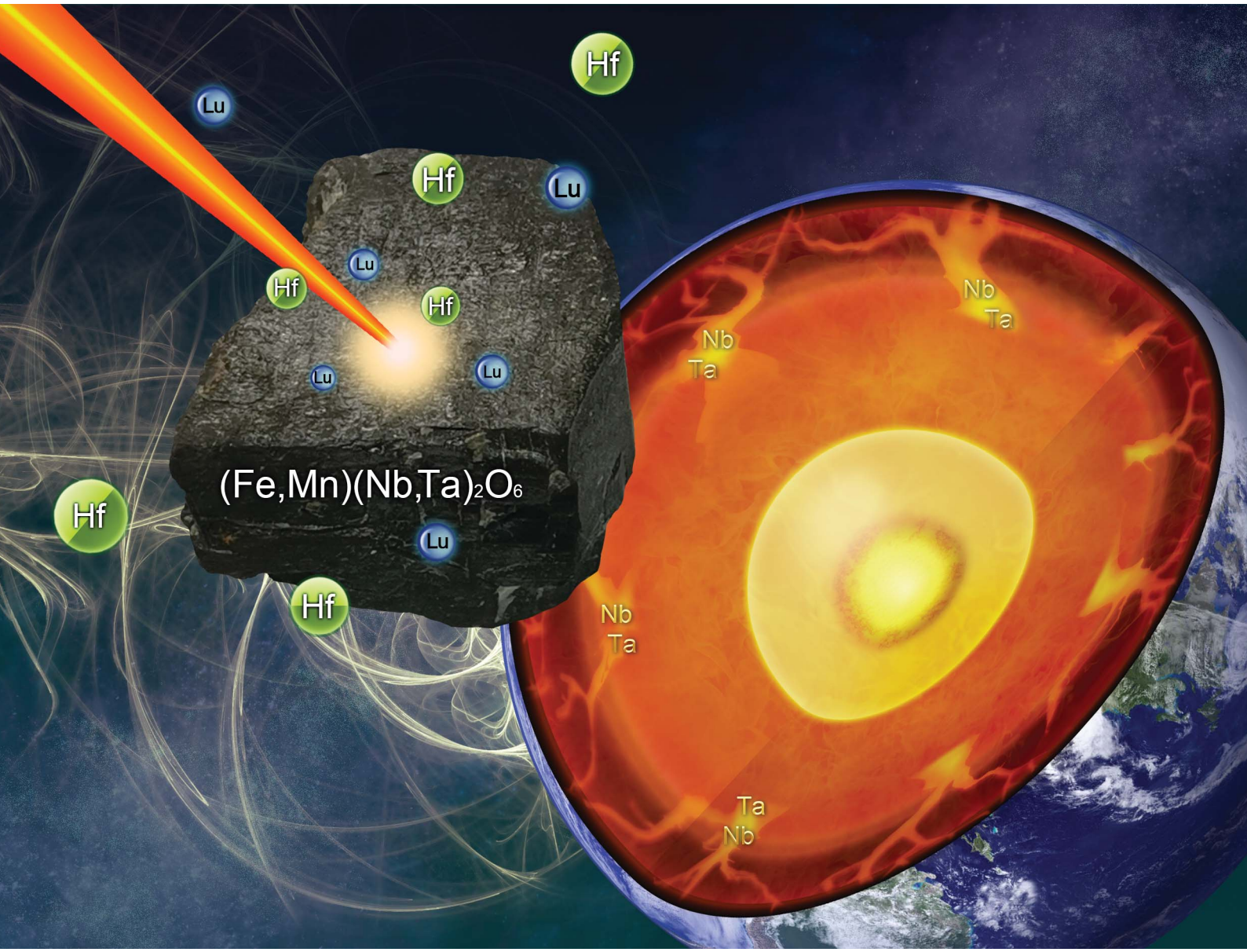

ISSN 0267-9477

ROYAL SOCIETY OF CHEMISTRY

PAPER

Xu-Dong Che, Yue-Heng Yang *et al.*
Precise and accurate Lu–Hf isotope analysis of columbite-group minerals by MC-ICP-MS

JAAS

ROYAL SOCIETY OF CHEMISTRY

PAPER

Cite this: *J. Anal. At. Spectrom.*, 2021, **36**, 1643

Precise and accurate Lu–Hf isotope analysis of columbite-group minerals by MC-ICP-MS†

Zhi-Min Tang,[a] Xu-Dong Che, *[a] Yue-Heng Yang, *[b] Fu-Yuan Wu,[b] Ru-Cheng Wang,[a] Jin-Hui Yang,[b] Axel Gerdes,[c] Ze-Ying Zhu,[d] Feng Liu[a] and Chang Zhang[b]

Due to their relatively high Hf contents (*i.e.*, several hundreds to thousands of ppm), columbite-group minerals (CGMs) are suitable for Lu–Hf isotope analysis, which can provide new insights into the source of such minerals in combination with the U–Pb age of rare-metal deposits. However, few studies have reported Lu–Hf isotope data for CGMs. Tantalum is a major element in CGMs (12–48 wt% Ta_2O_5) and has a significant effect on measurements of Hf isotopes using MC-ICP-MS. This effect was first evaluated in this study by analysis of mixed Hf–Ta standard solutions with different Ta/Hf ratios and LA-MC-ICP-MS analysis of various CGMs. This analytical artifact reflects serious tailing of the large ^{181}Ta signal onto the ^{180}Hf and ^{179}Hf masses during analysis. Therefore, in order to obtain accurate Hf isotope data for CGMs by MC-ICP-MS, we present an improved chemical separation procedure for Hf from Ta, and also a novel analytical protocol for LA-MC-ICP-MS analysis of CGMs. Accurate *in situ* $^{176}Hf/^{177}Hf$ ratios for CGMs can be obtained by normalization to $^{178}Hf/^{177}Hf = 1.4672$, rather than $^{179}Hf/^{177}Hf = 0.7325$, using the exponential law. This approach was validated by solution and laser ablation MC-ICP-MS analysis of four CGM samples from China and Africa. The Lu–Hf isotopic composition of CGMs provides a new geochemical tracer for rare-metal deposits.

Received 12th April 2021
Accepted 9th June 2021

DOI: 10.1039/d1ja00125f

rsc.li/jaas

1 Introduction

The Lu–Hf isotopic system is an important geochronometer and petrogenetic tracer in Earth sciences.[1,2] With improvements in multi-collector inductively coupled plasma mass spectrometry (MC-ICP-MS) and chemical separation procedures, the range of sample types suitable for Lu–Hf isotopic analysis has significantly expanded. Analysis of Lu–Hf isotopes by solution and laser ablation (LA)-MC-ICP-MS has been widely conducted on Hf-bearing minerals. Due to the high Hf contents of zircon (~0.5–2.0 wt%),[3] its Lu–Hf isotopic system is intensively studied. Zircon Hf isotopic ratios were determined accurately using LA-MC-ICP-MS as early as the mid-1990s to early 2000s.[4–7] As with zircon, the high Hf concentrations (~1.0–1.5 wt%)[8] of baddeleyite make it also suitable for Hf isotopic analyses. Since the 2000s, many studies of baddeleyite Hf isotopes were reported using solution and LA-MC-ICP-MS.[3,8–10] For eudialyte with Hf content of ~1000–4000 ppm,[11] Barfod *et al.*[12] firstly obtained Hf isotopes of eudialyte by solution MC-ICP-MS. After that, Kogarko *et al.*[13] and Wu *et al.*[11] used LA-MC-ICP-MS to measure its Hf isotopes in 2010. For Hf-poor rutile (usually <50 ppm),[14] its Hf isotopes were also measured by solution MC-ICP-MS and LA-MC-ICP-MS during the mid-2000s to 2010s.[14–16] Kendall-Langley *et al.*[17] recently undertook reconnaissance Lu–Hf isotope analysis of cassiterite (200–400 ppm Hf) by LA-MC-ICP-MS, which provided insights into Li–Cs–Ta pegmatite melts. However, there is no corresponding solution Lu–Hf isotope analysis of cassiterite.

Columbite-group minerals (CGMs) with the general formula $(Fe,Mn)(Nb,Ta)_2O_6$ are the most significant Nb- and Ta-bearing ore minerals, and occur mainly in rare-metal granitic, pegmatitic, alkali, and carbonatitic rocks.[18–21] The major and trace element chemistry of CGMs has been widely utilized in petrogenetic and geochemical studies.[18,22–27] CGMs have high U and low common Pb contents, and thus can be used for U–Pb dating.[26,28–34] Meanwhile, many CGMs have relatively high Hf contents (50–2650 ppm),[24,26,32,35–37] which makes these minerals suitable for Lu–Hf isotope studies. However, there is no established analytical protocol for CGMs. Recently, Marko *et al.*[38] briefly described Lu–Hf isotope analysis of CGMs by isotope dilution MC-ICP-MS in a conference abstract. The samples were collected by using a microdrill, and ε_{Hf} values of the same grain

[a]*State Key Laboratory for Mineral Deposits Research, School of Earth Sciences and Engineering, Nanjing University, Nanjing, 210023, China. E-mail: xdche@nju.edu.cn*
[b]*State Key Laboratory of Lithospheric Evolution, Institute of Geology and Geophysics, Chinese Academy of Sciences, Beijing, 100029, China. E-mail: yangyueheng@mail.iggcas.ac.cn*
[c]*Institut für Geowissenschaften, Goethe Universität Frankfurt, Altenhoeferallee 1, D-60438 Frankfurt am Main, Germany*
[d]*Tianjin Center of Geological Survey, CGS, Tianjin, 300170, China*

† Electronic supplementary information (ESI) available. See DOI: 10.1039/d1ja00125f

showed wide variation, which indicated that the Lu–Hf isotopic system of CGMs may be a potential petrogenetic tracer in the study of Nb–Ta mineralization. Nevertheless, there were no detailed chemical procedures for Hf isotope analysis of CGMs, and also there was no follow-up report.

It is difficult to accurately and precisely measure Hf isotopes using solution MC-ICP-MS and LA-MC-ICP-MS due to the following challenges: the first is how to effectively extract the Hf fraction from matrix elements by ion exchange methods. Münker *et al.*[39] separated Lu, Hf, and Ta from rock samples by a three-column separation procedure. However, Ta is the major element (wt% levels) in CGMs; it needs to be further investigated to elute the high concentration of Ta and extract pure Hf. The second is how to robustly correct mass bias for Hf. Generally speaking, mass bias is corrected using an exponential law, and the mass bias coefficient for Hf is traditionally calculated using $^{179}Hf/^{177}Hf = 0.7325$ in Hf isotope analysis.[3,4,9,14] However, tailing of ^{181}Ta on the low-mass side was reported which can seriously affect the signal on Hf in MC-ICP-MS.[40–42] Thus, mass bias needs to be further evaluated for *in situ* analysis of the CGM Hf isotope. The third is whether there is a matrix effect on Hf isotope measurements of CGMs. Considering that CGMs usually include ferrocolumbite, manganocolumbite, ferrotantalite, and manganotantalite subgroup minerals, with different Ta/(Nb + Ta) atomic ratios (abbreviated hereafter as $Ta^{\#}$) and Mn/(Fe + Mn) atomic ratios (abbreviated hereafter as $Mn^{\#}$), the matrix effect among different CGM endmembers during laser ablation should be examined and investigated in detail.

In this study we have developed the first robust methodology for Hf isotope analysis of CGMs. We undertook analysis of mixed Hf–Ta solutions and natural CGM samples and established an improved chemical procedure for Lu and Hf purification from CGMs for solution MC-ICP-MS analysis. We also established an analytical protocol of *in situ* Lu–Hf isotope analysis of CGMs by LA-MC-ICP-MS. Our novel protocols were validated by both solution and laser ablation MC-ICP-MS of four natural CGM samples from China and Africa. Our methodology will allow this isotopic system to be used as a tracer for rare-metal deposits.

2 Experimental procedures

2.1 Natural samples

Four CGM samples from different locations were analyzed in this study. One ferrotapiolite sample was also analyzed. Prior to Lu–Hf isotope analysis, back-scattered electron (BSE) images were obtained (Fig. 1) and quantitative elemental analyses (Fig. 2 and Table S1†) were performed by electron probe microanalysis (EPMA). Trace element contents (Table S1†) and *in situ* U–Pb ages (Table S2 and Fig. S1†) were determined by LA-ICP-MS. The detailed methods are described in Methods S1 and S2. Average Ta_2O_5, Nb_2O_5, Hf, Yb, and Lu contents for each sample are presented in Table 1. These samples are described briefly below.

NP-2 is a single black ferrocolumbite megacryst (approximately 50 × 20 × 10 mm) from the Nanping No. 31 pegmatite. The Nanping pegmatites are located 8 km west of Nanping City, Fujian Province, China. The Nanping No. 31 pegmatite is a highly differentiated and Nb–Ta–Sn-bearing dike. Rao *et al.*[43] described the petrography of this pegmatite dike. The dike has an LA-ICP-MS U–Pb CGM age of 387.1 ± 4.0 Ma,[44] and an ID-TIMS CGM age of 380.3 ± 2.4 Ma.[45]

U-1 and U-3 are single black manganocolumbite and ferrocolumbite megacrysts (approximately 25 × 10 × 5 mm), respectively, from an unknown location in Africa. These samples have LA-ICP-MS U–Pb ages of 971 ± 12 and 966 ± 12 Ma (this study), respectively.

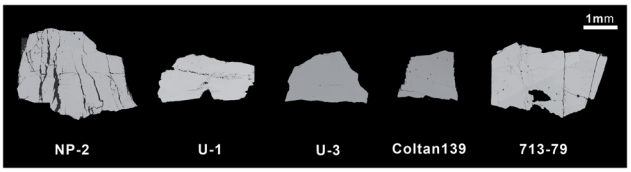

Fig. 1 Representative back-scattered electron (BSE) images of the CGM and ferrotapiolite grains.

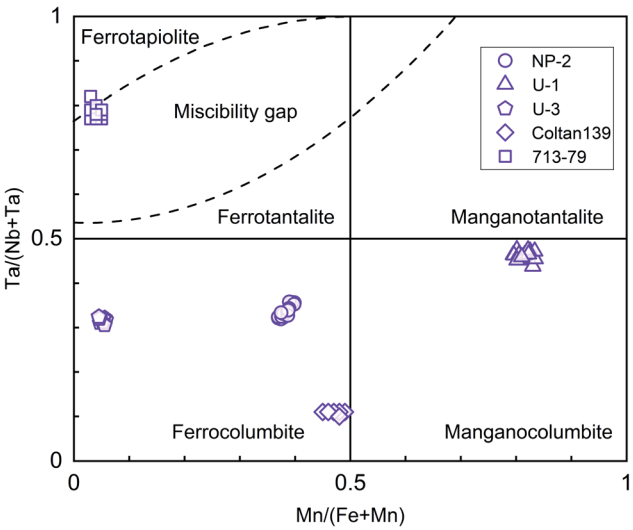

Fig. 2 Compositional plot of Ta/(Nb + Ta) *vs.* Mn/(Fe + Mn) for CGM and ferrotapiolite samples. Data for samples Coltan139 and 713-79 quoted from Che *et al.* (2015).[32]

Table 1 Selected major- and trace-element concentrations of the CGM and ferrotapiolite samples[a]

Sample	NP-2	U-1	U-3	Coltan139	713-79
Number	21	15	16	20	20
Ta_2O_5 (wt%)	36.65	47.78	34.55	12.67	65.71
Nb_2O_5 (wt%)	43.78	33.45	44.82	65.57	10.87
Number	32	27	25	30	20
Hf (ppm)	211	469	1430	454	712
Yb (ppm)	1.610	0.483	0.0804	95.4	0.017
Lu (ppm)	0.355	0.0681	0.0165	11.2	0.0043
Ta/Hf	1424	658	204	229	756
Nb/Hf	1452	3574	469	963	107

[a] Data of samples Coltan139 and 713-79 quoted from Che *et al.* (2015).[32]

Coltan139 is an external reference material for *in situ* U–Pb dating and elemental analysis of CGMs.[26,32–34,46] It is a single black ferrocolumbite megacryst (approximately 10 × 5 × 5 mm) from a pegmatite in Madagascar, Africa. ID-TIMS U–Pb dating of this sample has yielded an age of 505.4 ± 1.0 Ma.[26]

713-79 is a single black ferrotapiolite megacryst (approximately 20 × 10 × 5 mm) from the Altai Koktokay No. 3 pegmatite in Fuyun County, Xinjiang Province, China. The Altai Koktokay No. 3 pegmatite is an evolved dike. Zhang *et al.*[47] and Wang *et al.*[48] described the petrography of this dike, which has a LA-ICP-MS ferrotapiolite U–Pb age of 218 ± 2 Ma.[32]

2.2 Solution analysis

Chemical purification and mass spectrometry were undertaken at the State Key Laboratory of Lithospheric Evolution, Institute of Geology and Geophysics, Chinese Academy of Sciences (CAS), Beijing, and the State Key Laboratory for Mineral Deposits Research, Nanjing University (NJU), Nanjing, China. The chemical separation procedures were conducted in a class 100 laminar flow hood in a class 10 000 clean room environment. Samples NP-2, U-1, U-3, Coltan139, and 713-79 were subjected to solution Lu–Hf isotope analysis. We selected several small pieces from different parts of these samples for analysis.

2.2.1 Chemical reagents and materials. Milli-Q water (18.2 MΩ cm^{-1}) from Millipore (Elix-Millipore, USA) and hydrofluoric acid (HF), hydrochloric acid (HCl), nitric acid (HNO_3), perchloric acid ($HClO_4$), boric acid (H_3BO_3), and hydrogen peroxide (H_2O_2) were used for mineral digestion, elemental purification, and analysis. Spex Hf (1000 μg mL^{-1}) from SPEX CertiPrep, Alfa Hf (10 000 μg mL^{-1}) from Alfa Aesar of Johnson Matthey Company, and Ta solution (1000 μg mL^{-1}) from the National Analysis Center for Iron and Steel, China, were used to prepare mixed Hf–Ta solutions. Two chromatographic materials were used in our study, which were a Ln Spec cation exchange resin (100–150 μm particle size; 2 mL) from Eichrom Industries (Darien, Illinois, USA) and an AG 1-X8 anion exchange resin (200–400 mesh size; 2 mL) from Bio-Rad (Richmond, California; USA). Standard solutions of 200 ng mL^{-1} Alfa Hf, 50 ng mL^{-1} Alfa Lu, and 100 ng mL^{-1} JMC475 were prepared and used for the measurements. A series of mixed solutions with variable Ta/Hf ratios were analyzed (Table S3†). Standard reference materials BCR-2, BIR-1a, BHVO-2, and AGV-2 from the USGS were used to evaluate the chemical separation procedures.

2.2.2 Sample digestion. Handpicked and fresh CGM and ferrotapiolite grains were washed in Milli-Q water and ethanol before being powdered with an agate mortar and pestle. The digestion procedures for the CGM and ferrotapiolite samples were followed as described by Romer and Smeds[49] and Yang *et al.*[50] At CAS, approximately 10–20 mg of the sample powder and, in some cases, a mixed ^{176}Lu–^{180}Hf spike were weighed into 7 mL Savillex PFA vials, and then digested on a hot plate at 100 °C for one week in 22 M HF–14 M HNO_3–70% $HClO_4$ (2 mL + 1 mL + 0.2 mL). At NJU, approximately 20 mg of the sample powder was weighed into a bomb, and then dissolved in 0.2 mL of 70% $HClO_4$ and 4 mL of 29 M HF in an oven at 180 °C for one week.

The capsules were then opened and heated on a hot plate to dryness with fuming $HClO_4$. Subsequently, 1 mL of 6 M HCl was added to the residue and evaporated to dryness and then repeated. After the samples were evaporated to dryness and cooled, 5 mL of 3 M HCl + 3% H_3BO_3 were added to the residues. The capsules were resealed and placed on a hot plate at 80 °C for 12 h to dissolve the samples for chemical separation.

2.2.3 Column chemistry. Chemical separation of Hf from the mixed Hf–Ta solution and the natural samples was undertaken by ion exchange techniques. A two-column procedure was required for the separation procedure (Table 2). The first column was used to separate Lu and Hf (and Ta) from the matrix with the Ln Spec resin (Table 2). First, 2 mL of the Ln Spec resin was prepared in a mixture of 6 M HCl + 0.2 M HF and then preconditioned with 25 mL of 3 M HCl. In order to decrease the sample load, only 1.5–2.5 mL of the 5 mL solutions were loaded onto the first column. The matrix elements (including light rare earth elements) were sequentially eluted with 3 M and 4 M HCl. Both Lu and Yb were eluted with 5 mL of 4 M HCl, collected in a PFA beaker, and evaporated to dryness. This fraction was dissolved in a trace quantity of 3 M HCl and diluted with 0.5 mL of 2% HNO_3 before mass spectrometry. Subsequently, 6 M HCl was eluted through the column to remove any remaining Lu and Yb to minimize the isobaric interferences of ^{176}Lu and ^{176}Yb on ^{176}Hf. Titanium was eluted with a mixture of 4 M HCl + 0.5% H_2O_2. Finally, Hf–Ta was extracted with 4 mL of 2 M HF.

Given that Ta is a major element in the CGM and ferrotapiolite samples, a second column step was required to further separate Hf from Ta using an anion exchange resin (AG 1-X8; Table 2). First, 2 mL of the AG 1-X8 resin was prepared in 6 M HCl and Milli-Q H_2O, which was then preconditioned with 6 M HNO_3 + 0.2 M HF and 2 M HF. The Hf–Ta collected from the first column was loaded directly onto the second column. After eluting the matrix (mainly Ta) with 10 mL of 2 M HF, Hf was

Table 2 Two-column procedure for combined separation of Lu and Hf

Step	Column volumes	Acid
Column I (Ln Spec 2 mL *ca.* 0.8 cm × 4 cm)		
Preparation	20 mL × 3 times	6 M HCl + 0.2 M HF
Preconditioning	25 mL	3 M HCl
Loading sample	1.5–2.5 mL	3 M HCl
Eluting matrix	5 mL × 2 times	3 M HCl
Eluting matrix	5 mL × 2 times	4 M HCl
Collecting Yb, Lu	5 mL	4 M HCl
Eluting residual Yb, Lu	5 mL × 4 times	6 M HCl
Eluting Ti	20 mL	4 M HCl + 0.5% H_2O_2
Collecting Hf–Ta	4 mL	2 M HF
Column II (AG 1-X8 2 mL *ca.* 0.8 cm × 4 cm)		
Preparation	5 mL × 2 times	6 M HCl
	5 mL × 2 times	Milli-Q H_2O
Preconditioning	5 mL × 2 times	6 M HNO_3 + 0.2 M HF
	5 mL × 2 times	2 M HF
Loading Hf–Ta cut	4 mL	2 M HF
Eluting matrix	2.5 mL × 4 times	2 M HF
Collecting Hf	2 mL × 3 times	6 M HNO_3 + 0.2 M HF

collected in a PFA beaker in 6 mL of 6 M HNO_3 + 0.2 M HF, and evaporated to dryness. This residue was dissolved in trace amounts of 2 M HF and diluted to 1.25 mL with 2% HNO_3, and was then ready for Hf isotope analysis.

The mixed Hf–Ta solutions were divided into two parts. Separation of Hf from one aliquot was undertaken with the second column procedure described above, and the other aliquot was not purified. The mixed Spex Hf and Ta solutions were also not purified. After the spiked samples (U-1, U-3, Coltan139, and 713-79) were digested, these sample solutions were passed through the first column, and then the collected Hf (and Ta) was divided into two aliquots. One aliquot was passed through the second column, whereas the other was not.

2.2.4 Mass spectrometry. Lu–Hf isotope analyses were carried out using Thermo Fisher Scientific Neptune Plus MC-ICP-MS instruments at CAS and NJU, and the analytical methods were similar to those described by Yang *et al.*[50] The typical instrumental operating parameters and Faraday cup configurations are presented in Table 3. The interference from ^{176}Yb on ^{176}Lu was corrected by assuming that the mass bias behavior of Lu follows that of Yb and $^{176}Yb/^{172}Yb = 0.5887$ (using the exponential mass fractionation law). Hafnium isotope data were reduced offline and normalized to $^{179}Hf/^{177}Hf = 0.7325$ using the exponential law. Hafnium contents were calculated from the $^{180}Hf/^{177}Hf$ ratio using the isotope dilution method. During the period of data acquisition, standard reference materials were analyzed using the

Table 3 Operational parameters and Faraday cup configuration for the measurements of Lu and Hf isotopes[a]

MC-ICP-MS			
Lab.	CAS		NJU
Model	Thermo Fisher Scientific Neptune Plus		
RF forward power	~1200 W		~1200 W
Cooling gas	16 l min^{-1}		15 l min^{-1}
Auxiliary gas	0.8 l min^{-1}		0.95 l min^{-1}
Sample gas	1 l min^{-1}		
Extraction	−2000 V		
Focus	−620 V		
Detection system	Nine Faraday collectors		
Acceleration voltage	10 kV		
Interface cones	Standard cone		
Nebuliser type	Micromist PFA nebulise		
Sample uptake rate	50 μL min^{-1}		
Uptake mode	Free aspiration		
Resolution	~400 (low)		
Typical sensitivity	~16 V per ppm (10–11 Ω resistors) on 180Hf		
Sampling (solution)	9 blocks of 8 cycles for Hf 1 block of 30 cycles for Lu		4 blocks of 10 cycles for Hf
Sampling (laser)			1 blocks of 200 cycles for Hf
Integration time	4.194 s for Hf and 2.097 s for Lu (solution)		4.194 s (solution) or 0.131 s (laser) for Hf
Baseline	*ca.* 1 min on peak in 2% HNO_3		

Laser ablation system	
Lab.	NJU
Model	Geolas Pro MV2
Wave length	UV 193 nm
Energy density	~8 J cm^{-2}
Spot size	120 μm, 160 μm
Frequency	20 Hz

Faraday cup configuration

	L4	L3	L2	L1	Center	H1	H2	H3	H4
Solution									
Lu (CAS)	^{168}[Er + Yb]	^{170}[Er + Yb]	^{171}Yb	^{172}Yb	^{173}Yb	^{174}[Yb + Hf]	^{175}Lu	^{176}[Lu + Yb + Hf]	^{178}Hf
Hf (CAS)	^{173}Yb	^{175}Lu	^{176}[Hf + Yb + Lu]	^{177}Hf	^{178}Hf	^{179}Hf	^{180}[Hf + Ta + W]	^{181}Ta*	^{183}W
Hf (NJU)	^{172}Yb	^{174}Hf	^{175}Lu	^{176}Hf	^{177}Hf	^{178}Hf	^{179}Hf	^{180}[Hf + Ta]	
Laser									
Hf (NJU)	^{172}Yb	^{173}Yb	^{175}Lu	^{176}Hf	^{177}Hf	^{178}Hf	^{179}Hf	^{180}[Hf + Ta]	

[a] ^{181}Ta*: MC-ICP-MS did not accept the ^{181}Ta signal without purification by the second column, however accepted the ^{181}Ta signal when purified by the second column.

analytical procedures described above. The Hf isotope ratios of these reference materials agree well with published values for these standards (Table S4†).[2,50–54] In addition, $^{176}Hf/^{177}Hf$ ratios were normalized to $^{178}Hf/^{177}Hf = 1.4672$ using the exponential law for the standard Hf solutions doped with Ta, given that Ta has a significant effect on Hf isotope measurements.

2.3 *In situ* analysis

For laser ablation analyses, handpicked CGM and ferrotapiolite grains were mounted in epoxy resin and polished. The Lu–Hf isotope analyses for these samples were carried out at NJU using a Geolas Pro MV2 193 nm laser ablation system coupled to a Neptune Plus MC-ICP-MS. Table 3 lists the laser ablation system and MC-ICP-MS instrumental parameters. Both CGM and ferrotapiolite samples were analyzed using laser spot diameters of 120 μm for samples NP-2, U-1, and U-3, and 160 μm for samples Coltan139 and 713-79. The laser frequency was 20 Hz. The energy density was *ca.* 8 J cm^{-2}. The isobaric interferences from ^{176}Yb and ^{176}Lu on ^{176}Hf were calculated from the measured ^{172}Yb and ^{175}Lu intensities and natural ratios ($^{176}Yb/^{172}Yb = 0.5887$ and $^{176}Lu/^{175}Lu = 0.02655$). The very low Yb contents of the samples make it difficult to determine an accurate mass bias factor for Yb, and thus the mass bias for Yb was assumed to be the same as that for Hf. Instrumental mass bias for Hf was corrected based on the measured ^{179}Hf and ^{177}Hf intensities and the natural ratio ($^{179}Hf/^{177}Hf = 0.7325$) using the exponential law. The hafnium isotope ratios for a zircon reference material (91 500) obtained by LA-MC-ICP-MS agree well with the published values for this standard (Table S4†).[3,55] For comparison, $^{176}Hf/^{177}Hf$ ratios were also normalized to $^{178}Hf/^{177}Hf = 1.4672$ using the exponential law.

3 Results

3.1 Mixed Hf–Ta standard solutions

3.1.1 Purity of the Ta standard solution. To check the purity of the Ta standard solution used in this study, we measured the Hf signal of the 1000 and 10 000 ng mL^{-1} Ta standard solutions. The ^{178}Hf ion signals were very low (Table S5†), 0.00011 and 0.00024 V, respectively, whereas the ^{180}Hf intensities increased due to the contribution from Ta. The ^{177}Hf ion beam intensity from the 200 ng mL^{-1} Alfa Hf solution was ~1 V. By comparing the ^{177}Hf signal of the Alfa Hf and Ta solutions, approximate Hf concentrations of the Ta solutions were calculated (Table S5†), which were 0.015 ng mL^{-1} Hf in the 1000 ng mL^{-1} Ta solution and 0.033 ng mL^{-1} Hf in the 10 000 ng mL^{-1} Ta solution. This shows that the Ta standard solutions are almost Hf-free and high purity.

3.1.2 Hafnium isotopic compositions. Hafnium isotope data for the 50 ng mL^{-1} Spex Hf + Ta solutions and 200 ng mL^{-1} Alfa Hf + Ta solutions are shown in Fig. 3 (Table S6†). We prepared nine 200 ng mL^{-1} Alfa Hf solutions without Ta for analysis, and the obtained $^{176}Hf/^{177}Hf$ ratios are 0.282161–0.282178. A further 13 Hf solutions were doped with different amounts of Ta and analyzed after chemical separation on the second column, which yielded $^{176}Hf/^{177}Hf = 0.282173$–$0.282184$ with initial Ta/Hf ratios of 1–50. These results are the same as those for the 200 ng mL^{-1} Alfa Hf standard solution.[3]

Without the second column separation, the raw $^{176}Hf/^{177}Hf$ ratios of the mixed Hf–Ta solutions increased gradually away from the reference value with increasing Ta concentrations (Fig. 3). The $^{176}Hf/^{177}Hf$ values of the Spex Hf + Ta solutions (0.282150–0.282353), with Ta/Hf = 1–60, deviate from the reference value ($^{176}Hf/^{177}Hf = 0.282160 \pm 20$; in-house NJU Hf standard) when Ta/Hf ≥ 10 ($^{176}Hf/^{177}Hf = 0.282187 \pm 13$ when Ta/Hf = 10). The $^{176}Hf/^{177}Hf$ values of the Alfa Hf + Ta solutions (0.282169–0.282250), with Ta/Hf = 1–50, deviate from the reference value when Ta/Hf ≥

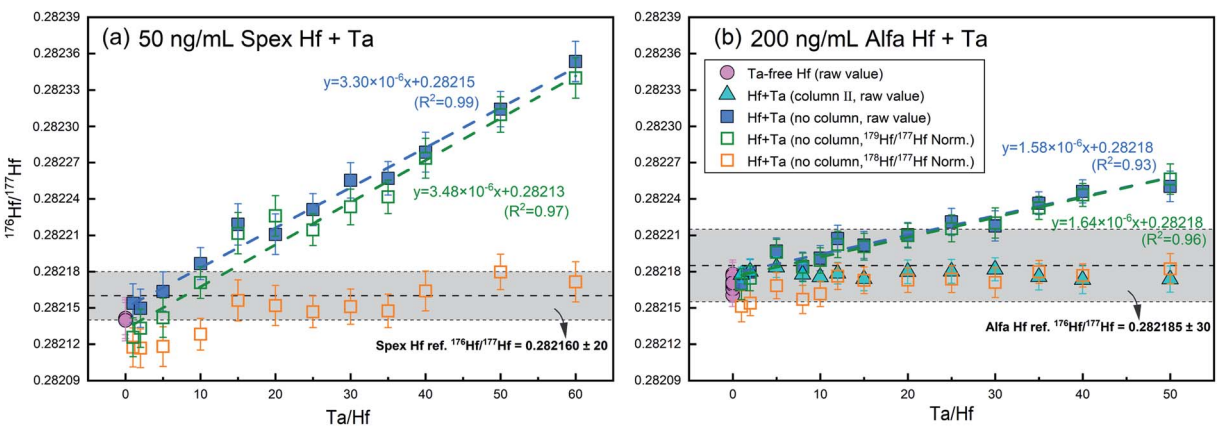

Fig. 3 $^{176}Hf/^{177}Hf$ values of the mixed Ta–Hf standard solutions. (a) 50 ng mL^{-1} Spex Hf + Ta solutions; (b) 200 ng mL^{-1} Alfa Hf + Ta solutions. Error bars are 2SE values for the individual analyses. Shaded areas are the $^{176}Hf/^{177}Hf$ reference value of Alfa Hf (0.282185 ± 30; in-house CAS standard) and Spex Hf (0.282160 ± 20; in-house NJU standard). Blue dotted lines are the best-fit lines through the Hf isotope ratios measured on the 50 ng mL^{-1} Spex Hf + Ta and 200 ng mL^{-1} Alfa Hf + Ta solutions that were not passed through the second column. Green dotted lines are the best-fit lines through their Hf isotope ratios without chemical separation but reduced offline by normalization to $^{179}Hf/^{177}Hf = 0.7325$ using the exponential law. Pink circles are the raw $^{176}Hf/^{177}Hf$ ratios of the Ta-free Hf solutions. Orange squares are Hf isotopic data for the mixed Hf–Ta solution that were analyzed without chemical separation but reduced offline by normalization to $^{178}Hf/^{177}Hf = 1.4672$ using the exponential law. Solid triangles are raw $^{176}Hf/^{177}Hf$ ratios of the Alfa Hf + Ta solution that was passed through both columns.

Table 4 Comparison of the Lu–Hf isotopic compositions of spiked and unspiked CGM and ferrotapiolite samples measured using MC-ICP-MS between one- and two-stage chemical purification[a]

	Column I + II (Ln resin + AG1-X8 resin) (Hf separation from Ta matrix)							Column I (Ln resin) (Hf unseparation from Ta matrix)					
Sample	Split 1	Lu (μg g^{-1})	Hf (μg g^{-1})	$^{176}Lu/^{177}Hf$	$^{176}Hf/^{177}Hf$ (±2SE)	$^{176}Hf/^{177}Hf$*(±2SE)	$\varepsilon_{Hf(t)}$(±2SE)	Split 2	Lu (μg g^{-1})	Hf (μg g^{-1})	$^{176}Lu/^{177}Hf$	$^{176}Hf/^{177}Hf$(±2SE)	$\varepsilon_{Hf(t)}$(±2SE)
NP-2-1	1-1a	0.310	247	0.000178	0.282151(37)	0.282147(05)^{NJU}	−13.5(1.3)						
NP-2-2	2-1a	0.366	233	0.000223	0.282190(18)		−12.1(0.6)						
NP-2-3	3-1a	0.311	291	0.000152	0.282168(24)	0.282152(05)^{NJU}	−12.9(0.9)						
NP-2-4	4-1a	0.249	194	0.000182	0.282164(21)	0.282149(07)^{NJU}	−13.0(0.7)						
Mean[±2SD]				**0.000184[059]**	**0.282169[32]**		**−12.9[1.1]**						
U-1-1						0.281855(20)^{NJU}							
U-1-2	2-1a	0.0203	262	0.000011	0.281862(26)		−10.7(0.9)	2-1b	0.0203	262	0.000028	0.293950(74)	417.7(2.6)
U-1-3	3-1a	0.0311	175	0.000025	0.281824(44)		−12.1(1.6)	3-1b	0.0311	175	0.000050	0.297876(71)	556.8(2.5)
U-1-4	4-1a	0.0192	360	0.000008	0.281848(20)		−11.2(0.8)	4-1b	0.0192	360	0.000010	0.284152(31)	70.4(1.1)
Mean[±2SD]				**0.000015[019]**	**0.281845[38]**		**−11.3[1.4]**				**0.000030[40]**	**0.291993[14 137]**	**348.3[501.0]**
U-3-1	1-1a	0.0609	667	0.000013	0.281712(7)		−16.1(0.4)	1-1b	0.0609	560	0.000015	0.282346(22)	6.3(0.8)
U-3-2	2-1a	0.0362	510	0.000010	0.281717(7)		−16.0(0.4)	2-1b	0.0362	363	0.000014	0.282553(31)	13.6(1.1)
	2-2a	0.0218	523	0.000006	0.281691(11)		−16.9(0.5)						
U-3-3	3-1a	0.0383	681	0.000008	0.281693(10)	0.281694(04)^{NJU}	−16.8(0.5)	3-1b	0.0526	589	0.000013	0.282371(24)	7.2(0.9)
Mean[±2SD]				**0.000009[006]**	**0.281703[26]**		**−16.5[0.9]**				**0.000014[003]**	**0.282423[226]**	**9.0[8.0]**
Coltan139-1	1-1a	7.715	314	0.003495	0.281992(12)	0.281998(03)^{NJU}	−17.6(0.4)	1-1b	7.715	227	0.004837	0.282014(47)	−17.3(1.7)
Coltan139-2	2-1a	7.772	307	0.003596	0.281991(10)		−17.7(0.4)	2-1b	7.772	260	0.004245	0.282044(46)	−16.0(1.6)
Coltan139-3	3-1a	7.907	307	0.003663	0.281990(10)		−17.8(0.4)	3-1b	7.907	270	0.004168	0.282049(35)	−15.8(1.2)
Mean[±2SD]				**0.003585[168]**	**0.281991[03]**		**−17.7[0.2]**				**0.004417[733]**	**0.282036[38]**	**−16.4[1.6]**
713-79-1	1-1a	0.0239	346	0.000010	0.282762(08)	0.282732(07)	4.4(0.3)	1-1b	0.0239	324	0.000010	0.283099(16)	16.4(0.6)
713-79-2	2-1a	0.0425	189	0.000032	0.282740(10)	0.282738(08)	3.7(0.4)	2-1b	0.0425	129	0.000047	0.282800(69)	5.8(2.4)
	2-2a	0.0343	184	0.000026	0.282743(11)		3.7(0.4)						
713-79-3	3-1a	0.0264	333	0.000011	0.282765(05)	0.282767(06)	4.5(0.2)	3-1b	0.0264	284	0.000013	0.283050(17)	14.6(0.6)
	3-2a	0.0181	329	0.000008	0.282733(06)		3.4(0.2)						
Mean[±2SD]				**0.000017[022]**	**0.282749[28]**		**4.0[1.0]**				**0.000024[041]**	**0.282983[321]**	**12.2[11.4]**

[a] 2SE means 2 standard errors of the individual analysis. 2SD means 2 standard deviation on the mean of multiple analyses. $^{176}Hf/^{177}Hf$* means unspiked data, ^{NJU}: means measurement at NJU, other measurements at CAS.

25 ($^{176}Hf/^{177}Hf = 0.282221 \pm 11$ when Ta/Hf = 25). The $^{176}Hf/^{177}Hf$ and Ta/Hf ratios exhibit a strong linear correlation ($R^2 = 0.99$ and 0.93, respectively), but the slopes of the two correlations are different (slope = 3.30×10^{-6} and 1.58×10^{-6}, respectively).

The $^{176}Hf/^{177}Hf$ ratios of the mixed solutions without the second column purification were reduced offline and normalized to $^{179}Hf/^{177}Hf = 0.7325$ using the exponential law. The result is similar to the raw value above (Fig. 3). There is a strong linear correlation between $^{176}Hf/^{177}Hf$ and Ta/Hf ratios ($R^2 = 0.97$ for Spex and 0.96 for Alfa, respectively); the slopes of the two correlations are also different (slope = 3.48×10^{-6} and 1.64×10^{-6}, respectively).

The $^{176}Hf/^{177}Hf$ ratios of the mixed solutions without the second column separation were reduced offline and normalized to $^{178}Hf/^{177}Hf = 1.4672$ using the exponential law. The $^{176}Hf/^{177}Hf$ ratios for the Spex Hf + Ta solutions are 0.282117–0.282180, with Ta/Hf = 1–60 (Fig. 3a), which are consistent with the Spex Hf isotopic reference value. For the Alfa Hf + Ta solutions, $^{176}Hf/^{177}Hf$ ratios vary from 0.282151–0.282182 with Ta/Hf = 1–50 (Fig. 3b), which agree well with the Alfa Hf isotopic reference value. As such, accurate $^{176}Hf/^{177}Hf$ ratios can be determined for mixed Hf–Ta standard solutions by normalization to $^{178}Hf/^{177}Hf = 1.4672$.

3.2 Natural samples

3.2.1 Solution analyses. The Lu and Hf contents and Hf isotopic compositions for samples NP-2, U-1, U-3, Coltan139, and 713-79 are listed in Table 4 and shown in Fig. 4. The Hf

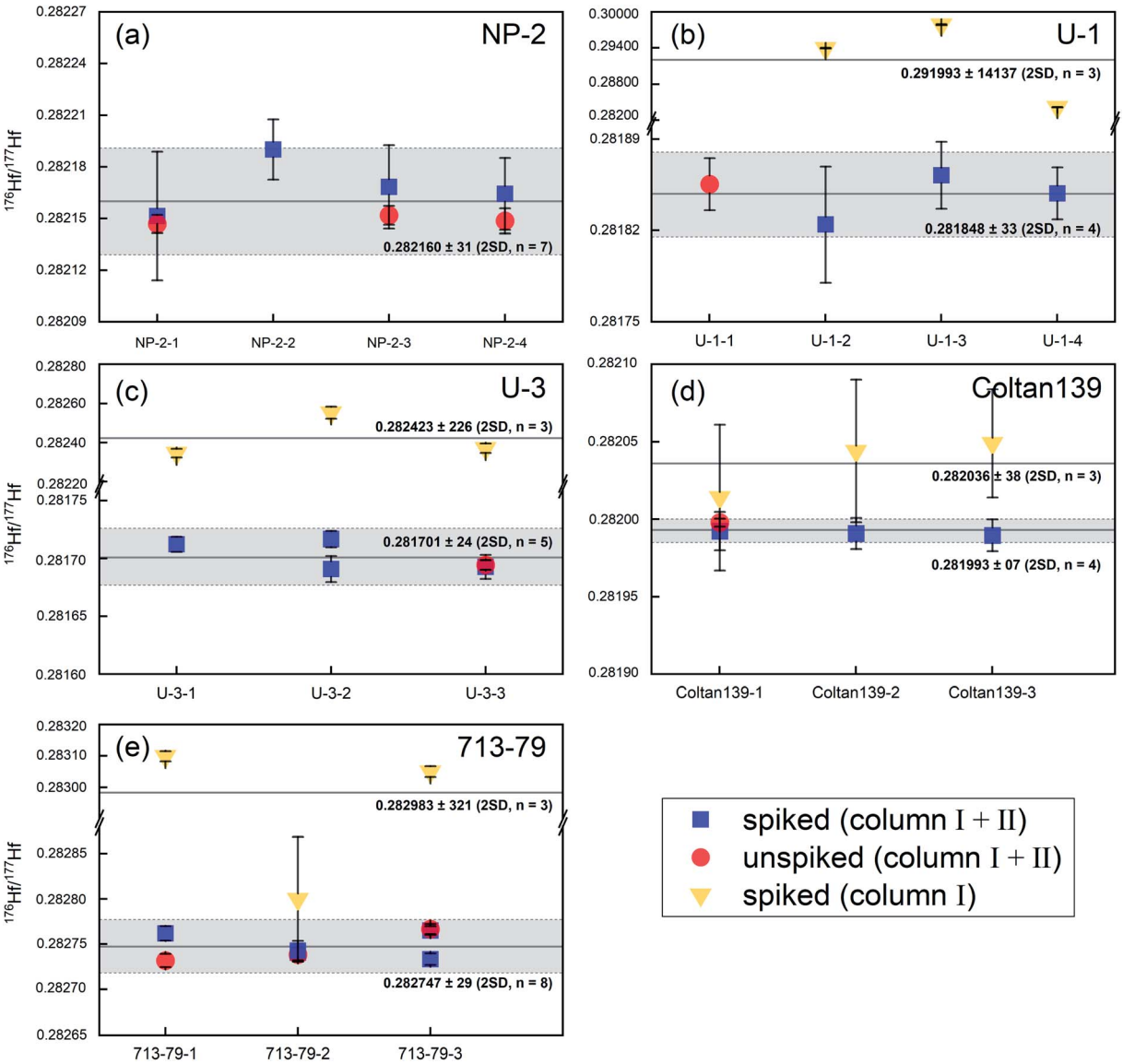

Fig. 4 $^{176}Hf/^{177}Hf$ ratios of the CGM and ferrotapiolite samples measured by MC-ICP-MS. Error bars are the 2SE values for the individual analyses. The gray box is the two standard deviation (2SD) field of the mean of multiple analyses of spiked and unspiked samples after passing through both columns. Blue squares and red dots are $^{176}Hf/^{177}Hf$ ratios of spiked and unspiked samples after passing through both columns. Yellow triangles are $^{176}Hf/^{177}Hf$ ratios of the spiked sample after passing through the first column.

isotope ratios obtained with or without spiking for each CGM and ferrotapiolite sample are the same. For sample NP-2, all of the Hf isotopic compositions are identical within analytical precision, with a mean value of $^{176}Hf/^{177}Hf = 0.282160 \pm 0.000031$ (2SD; $n = 7$). For sample U-1, the calculated mean $^{176}Hf/^{177}Hf = 0.281848 \pm 0.000033$ (2SD; $n = 4$). The Hf isotopic data for U-3 yield a mean value of $^{176}Hf/^{177}Hf = 0.281701 \pm 0.000024$ (2SD; $n = 5$). For Coltan139, $^{176}Hf/^{177}Hf = 0.281993 \pm 0.000007$ (2SD; $n = 4$). Sample 713-79 yielded a mean $^{176}Hf/^{177}Hf = 0.282747 \pm 0.000029$ (2SD; $n = 8$). The calculated mean $\varepsilon_{Hf(t)}$ values are -12.9 ± 1.1 (2SD; $n = 4$) for NP-2, -11.3 ± 1.4 (2SD; $n = 3$) for U-1, -16.5 ± 0.9 (2SD; $n = 4$) for U-3, -17.7 ± 0.2 (2SD; $n = 3$) for Coltan139, and 4.0 ± 1.0 (2SD; $n = 5$) for 713-79.

Some spiked samples (U-1, U-3, Coltan139, and 713-79) were chemically separated using only the first column, and the results are listed in Table 4 and shown in Fig. 4. The MC-ICP-MS analyses yielded $^{176}Hf/^{177}Hf$ values with a mean of 0.291993 ± 0.014137 (2SD; $n = 3$) for U-1, 0.282423 ± 0.000226 (2SD; $n = 3$) for U-3, 0.282036 ± 0.000038 (2SD; $n = 3$) for Coltan139, and 0.282983 ± 0.00321 (2SD; $n = 3$) for 713-79. The mean $\varepsilon_{Hf(t)}$ values are 348.3 ± 501.0 (2SD; $n = 3$) for U-1, 9.0 ± 8.0 (2SD; $n = 3$) for U-3, -16.4 ± 1.6 (2SD; $n = 3$) for Coltan139, and $12.2 \pm$

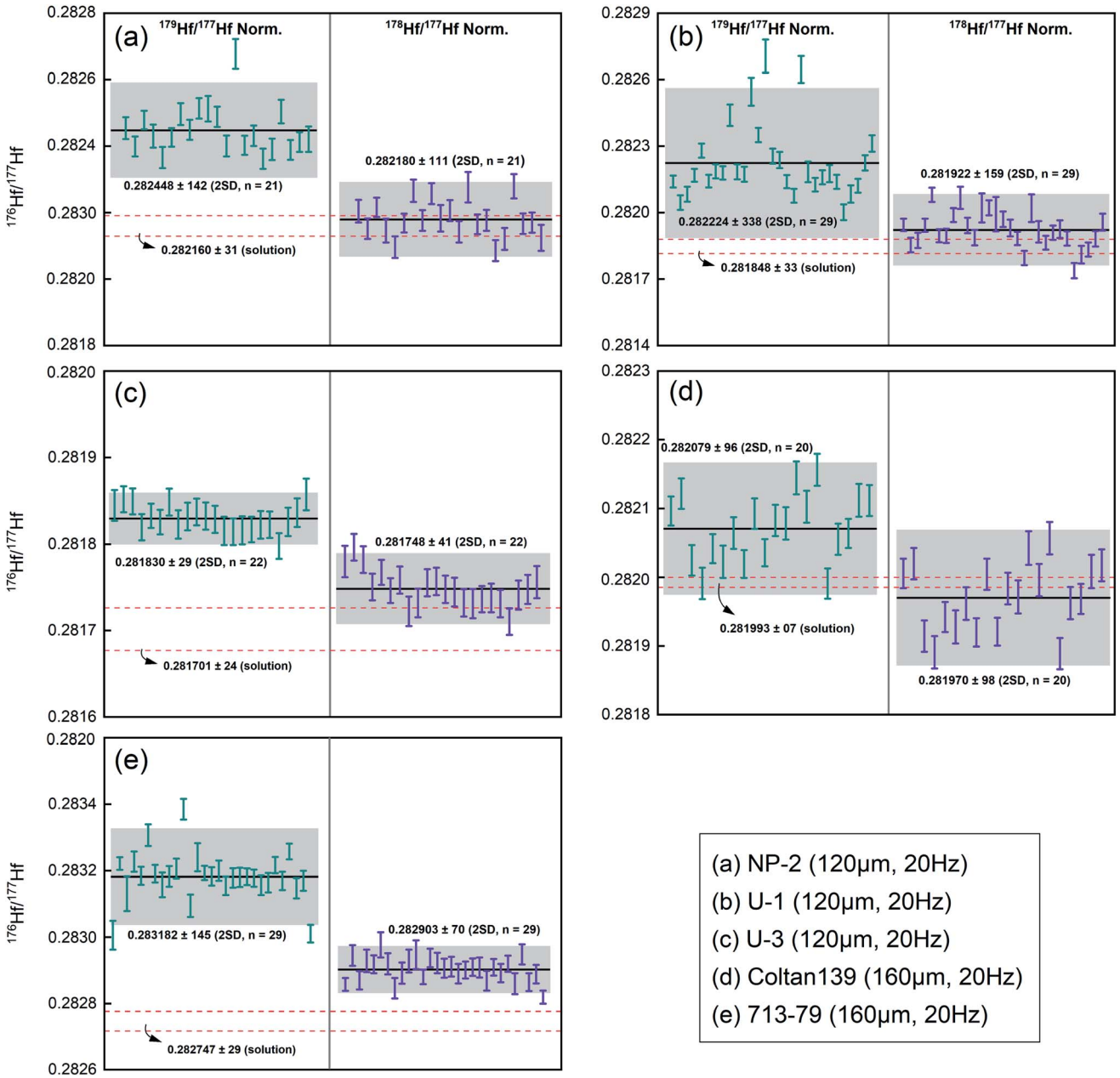

Fig. 5 *In situ* $^{176}Hf/^{177}Hf$ measurements of the CGM and ferrotapiolite samples using different normalization schemes. Blue points represent data normalized to $^{179}Hf/^{177}Hf = 0.7325$. Purple points represent data normalized to $^{178}Hf/^{177}Hf = 1.4672$. The black line is the mean of the Hf isotope analyses. The gray box highlights the 2SD range on the mean $^{176}Hf/^{177}Hf$ value obtained by LA-MC-ICP-MS. The red dotted line is the range of $^{176}Hf/^{177}Hf$ values obtained using the solution method.

11.4 (2SD; $n = 3$) for 713-79. However, these $^{176}Hf/^{177}Hf$ ratios are higher than those of the corresponding solutions that were chemically separated through two-step column procedures.

3.2.2 *In situ* analyses. *In situ* Hf isotope data for the five natural samples (NP-2, U-1, U-3, Coltan139, and 713-79) are shown in Fig. 5 (Tables S7 and S8†). A comparison between the solution and laser ablation analyses is provided in Table 5.

Using $^{179}Hf/^{177}Hf = 0.7325$ for normalization, the CGM and ferrotapiolite samples yielded the following mean $^{176}Hf/^{177}Hf$ values: 0.282448 ± 0.000142 (2SD; $n = 21$) for NP-2, 0.282224 ± 0.000338 (2SD; $n = 29$) for U-1, 0.281830 ± 0.000029 (2SD; $n = 22$) for U-3, 0.282079 ± 0.000096 (2SD; $n = 20$) for Coltan139, and 0.283182 ± 0.000145 (2SD; $n = 29$) for 713-79. The calculated mean $\varepsilon_{Hf(t)}$ values are −3.0 ± 5.0 (2SD; $n = 21$) for NP-2, 2.1 ± 2.0 (2SD; $n = 29$) for U-1, −12.0 ± 1.0 (2SD; $n = 22$) for U-3, −14.6 ± 3.4 (2SD; $n = 20$) for Coltan139, and 19.3 ± 2.1 (2SD; $n = 29$) for 713-79. These $^{176}Hf/^{177}Hf$ ratios are higher than those obtained using the solution methods.

In contrast, using $^{178}Hf/^{177}Hf = 1.4672$ for normalization, these samples yielded the following mean $^{176}Hf/^{177}Hf$ values: NP-2 = 0.282180 ± 0.000111 (2SD; $n = 21$), U-1 = 0.281922 ± 0.000159 (2SD; $n = 29$), U-3 = 0.281748 ± 0.000041 (2SD; $n = 22$), Coltan139 = 0.281970 ± 0.000098 (2SD; $n = 20$), and 713-79 = 0.282903 ± 0.000070 (2SD; $n = 29$). The mean $\varepsilon_{Hf(t)}$ values are −12.5 ± 3.9 (2SD; $n = 21$) for NP-2, −8.6 ± 5.6 (2SD; $n = 29$) for U-1, −14.9 ± 1.4 (2SD; $n = 22$) for U-3, −18.4 ± 3.5 (2SD; $n = 20$) for Coltan139, and 9.4 ± 2.5 (2SD; $n = 29$) for 713-79. The $^{176}Hf/^{177}Hf$ values for samples Coltan139 and NP-2 agree with their solution analyses. The $^{176}Hf/^{177}Hf$ values of samples U-1 and U-3 are very close to those determined by solution analysis. However, the $^{176}Hf/^{177}Hf$ ratio and $\varepsilon_{Hf(t)}$ value of sample 713-79 are totally inconsistent with those determined by solution methods; the probable reason will be discussed in other sections.

4 Discussion

4.1 Influence of Ta on Hf isotope measurements

From the perspective of mass spectrometry, the abundance sensitivity is one of the most important indices to characterize the influence of a strong peak on a nearby weak peak.[56] Peak tailing of a high-abundance isotope on neighboring masses can lead to the determination of inaccurate isotope ratios.[57–59] It was previously shown that tailing of ^{181}Ta on the low-mass side can seriously affect the signal on Hf in MC-ICP-MS.[40–42] The two isotopes of tantalum are ^{180}Ta (0.012%) and ^{181}Ta (99.99%). CGM and ferrotapiolite normally have very high Ta contents ($Ta_2O_5 \geq 12.67\%$; this study). In our experiments, the Ta signal could not be collected in a Faraday cup during both the solution (as Ta was not removed) and *in situ* measurements. For the mixed Alfa Hf + Ta standard solution, the measured $^{176}Hf/^{177}Hf$ values without removing Ta are higher than those obtained after chemical purification (Fig. 3). For the natural samples, the measured $^{176}Hf/^{177}Hf$ values after chemical separation using only the Ln Spec resin are higher than those after using both columns (Fig. 4), and the *in situ* Hf isotopic data (normalization to $^{179}Hf/^{177}Hf = 0.7325$) are higher than those obtained using

Table 5 Comparison of the Lu–Hf isotopic compositions of the CGM and ferrotapiolite samples measured using MC-ICP-MS between solution and laser sampling

Sample	$^{176}Lu/^{177}Hf$	$^{176}Hf/^{177}Hf$[±2SD]	$\varepsilon_{Hf(t)}$[±2SD]	n	Norm.	Methods	Remarks	$^{176}Lu/^{177}Hf$	$^{176}Hf/^{177}Hf$[±2SD]	$\varepsilon_{Hf(t)}$[±2SD]	n	Norm.	Methods	Remarks
NP-2	0.000184[059]	0.282169[32]	−12.9[1.1]	4		Solution	Two-stage						Solution	One-stage
	0.000250[021]	0.282180[111]	−12.5[3.9]	21	$^{178}Hf/^{177}Hf$	Laser		0.000250[021]	0.282448[142]	−3.0[5.0]	21	$^{179}Hf/^{177}Hf$	Laser	
U-1	0.000015[019]	0.281845[38]	−11.3[1.4]	3		Solution	Two-stage	0.000030[40]	0.291993[14 137]	348.3[501.0]	3		Solution	One-stage
	0.000037[013]	0.281922[159]	−8.6[5.6]	29	$^{178}Hf/^{177}Hf$	Laser		0.000037[013]	0.282224[338]	2.1[12.0]	29	$^{179}Hf/^{177}Hf$	Laser	
U-3	0.000009[006]	0.281703[26]	−16.5[0.9]	4		Solution	Two-stage	0.000014[003]	0.282423[226]	9.0[8.0]	3		Solution	One-stage
	0.000010[052]	0.281748[41]	−14.9[1.4]	22	$^{178}Hf/^{177}Hf$	Laser		0.000010[052]	0.281830[29]	−12.0[1.0]	22	$^{179}Hf/^{177}Hf$	Laser	
Coltan139	0.003585[168]	0.281991[03]	−17.7[0.2]	3		Solution	Two-stage	0.004417[733]	0.282036[38]	−16.4[1.6]	3		Solution	One-stage
	0.003410[077]	0.281970[98]	−18.4[3.5]	20	$^{178}Hf/^{177}Hf$	Laser		0.003415[077]	0.282079[96]	−14.6[3.4]	20	$^{179}Hf/^{177}Hf$	Laser	
713-79	0.000017[022]	0.282749[28]	4.0[1.0]	5		Solution	Two-stage	0.000024[041]	0.282983[321]	12.2[11.4]	3		Solution	One-stage
	0.000021[034]	0.282903[70]	9.4[2.5]	29	$^{178}Hf/^{177}Hf$	Laser		0.000021[034]	0.283182[145]	19.3[5.1]	29	$^{179}Hf/^{177}Hf$	Laser	

the solution method after the two-column purification. These results indicate that high Ta contents have a significant effect on the Hf isotope measurements. The mass bias factor for Hf is generally calculated using $^{179}Hf/^{177}Hf = 0.7325$. However, if the Ta content is sufficiently high, the weak ^{179}Hf peak can be seriously affected by the Ta tail. Therefore, an incorrect mass bias factor is calculated, which results in erroneously high $^{176}Hf/^{177}Hf$ values. But using $^{178}Hf/^{177}Hf = 1.4672$ results in accurate Hf isotopic data for the CGMs (Ta_2O_5 up to 47.78 wt%; this study). Nevertheless, for ferrotapiolite, its Ta content is very high (*e.g.*, the Ta_2O_5 content of sample 713-79 is as high as 65.71 wt%). So the reason is likely to be that during Hf isotope analysis using LA-MC-ICP-MS, the strong peak tailing from Ta might even affect ^{178}Hf and result in inaccurate Hf isotope ratios.

The slopes of the two correlations in Fig. 3 are significantly different; they are likely to be affected by the concentration of Hf and Ta in the solution, mainly controlled by the Hf concentration. During the Hf isotope measurements, the higher the concentration of Hf, the higher the signal value of Hf obtained, and the lower the effect of Ta tailing (even with relatively high Ta content) achieved. Thus, the significantly different slopes of the two correlations in Fig. 3 show that it is difficult to correct laser data by the standard solution method. Boulyga and Becker[60] have proposed that peak tailing can be reduced by an He-filled collision cell. Therefore, it is possible that a collision cell could reduce the peak tailing from Ta on Hf, and produce accurate Hf isotope data for ferrotapiolite.

4.2 Method validation

Ln Spec resin is widely used to separate Lu and Hf from rock and some mineral samples in a single purification step.[14,39,50,61] HF is a suitable elution medium for high field strength elements because of their low distribution coefficients with Ln Spec resin in 2 M HF.[39] For the CGM and ferrotapiolite samples with high concentrations of Ta, the Hf solution collected from the Ln Spec resin column still contains a large amount of Ta, and thus needs further purification. We determined the $^{176}Hf/^{177}Hf$ ratios of the mixed Alfa Hf and Ta solutions using MC-ICP-MS after passing these through the AG 1-X8 resin column and evaluated the Ta removal efficiency of the resin. The acid used for sample loading on the second column is 2 M HF, because Hf and Ta are retained on the column in 2 M HF.[62] In order to separate Ta and Hf from the solution, a 6 M HNO_3 + 0.2 M HF mixture can be used to extract Hf, but Ta is still strongly absorbed on the resin.[63] The Alfa Hf isotope data for the mixed Hf–Ta solutions obtained by MC-ICP-MS are in good agreement with their reference value (Fig. 3b), which demonstrates that the AG 1-X8 resin column can effectively separate Hf from Ta.

There have been many Hf isotope studies of zircon. Zircon often coexists with CGMs and ferrotapiolite in rare-metal granites and pegmatites, and has textural characteristics indicative of the coeval crystallization of these minerals.[64,65] We compiled Hf isotopic data for zircons from the same areas (Nanping No. 31 and Koktokay No. 3 pegmatites) from the literature for comparison with those obtained by (LA)-MC-ICP-MS analysis of CGMs and ferrotapiolite in this study. The zircon $\varepsilon_{Hf(t)}$ values of the Nanping No. 31 pegmatite range from −13.81 to −11.60 with TC DM model ages of 2107 to 2246 Ma.[44] The zircon $\varepsilon_{Hf(t)}$ values of the Koktokay No. 3 pegmatite vary from 0.80 to 2.39 with TC DM model ages of 973 to 1173 Ma.[64,66] The good agreement of $\varepsilon_{Hf(t)}$ values and model ages between the studied samples (NP-2 and 713-79 from Nanping and Koktokay, respectively) and zircon demonstrates that Lu–Hf isotope data can be measured accurately for CGM and ferrotapiolite samples using the solution method presented here (Table S9† and Fig. 6).

The Hf isotopic compositions of each of the samples (U-1, U-3, Coltan139, and 713-79) measured by MC-ICP-MS after one-stage purification are quite different from those after two-stage purification, which indicates that the AG 1-X8 resin column can remove large amounts of Ta from natural samples. The excellent reproducibility of the solution method is evident from the multiple analyses of samples NP-2, U-1, U-3, Coltan139, and 713-79 (unspiked or spiked) in two laboratories (CAS and NJU), which yielded consistent $^{176}Hf/^{177}Hf$ ratios. These CGM and ferrotapiolite samples from each of the areas have basically the same $\varepsilon_{Hf(t)}$ values and model ages. Moreover, individual $^{176}Hf/^{177}Hf$ measurements have small errors (2SE values are mainly <0.000030), and the corresponding error in the $\varepsilon_{Hf(t)}$ value is also low (2SE values are mainly <1). This indicates that the measurement accuracy is excellent for the solution method.

For normalization to $^{178}Hf/^{177}Hf = 1.4672$, the Hf isotopic compositions measured by LA-MC-ICP-MS are in agreement with those measured by solution MC-ICP-MS for NP-2, U-1, U-3, and Coltan139. This shows that Hf isotopes can be measured accurately for CGMs using the laser ablation protocol presented here. The precision attained by LA-MC-ICP-MS is a bit worse than that obtained by solution MC-ICP-MS, but it is sufficient to

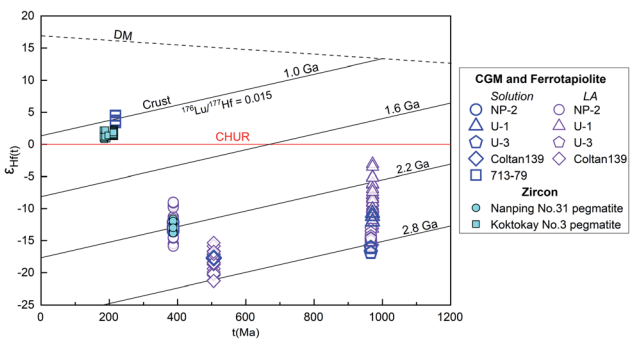

Fig. 6 Plot of age *versus* $\varepsilon_{Hf(t)}$ for the studied samples and zircons. The studied samples were analyzed using (LA)-MC-ICP-MS. DM = depleted mantle; CHUR = chondritic uniform reservoir; 1.0, 1.6, 2.2, and 2.8 Ga are the Hf isotope evolution lines for crust newly generated at 1.0, 1.6, 2.2, and 2.8 Ga, respectively. The ages for NP-2, Coltan139, and 713-79 are from Tang *et al.* (2017),[44] Melcher *et al.* (2015),[26] and Che *et al.* (2015),[32] respectively. The ages for U-1 and U-3 were obtained in this study. The age and Hf isotopic compositions of zircon from the Nanping No. 31 pegmatite are from Tang *et al.* (2017),[44] and those for the Altai Koktokay No. 3 pegmatite are from Zhou (2013)[72] and Chen *et al.* (2018).[66]

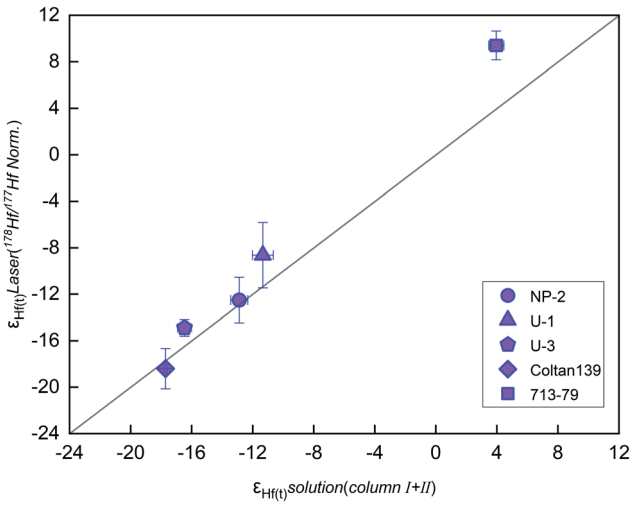

Fig. 7 Mean $\varepsilon_{Hf(t)}$ values of CGM and ferrotapiolite samples measured by MC-ICP-MS using solution and laser ablation methods. The error bars represent the 1SD values for individual analyses. The data obtained by the solution method are after the samples had been passed through both columns, and the data obtained using the laser ablation method were normalized to $^{178}Hf/^{177}Hf = 1.4672$.

distinguish the $^{176}Hf/^{177}Hf$ values of the different CGM samples. The mean Hf isotope ratios from multiple analyses of CGMs obtained by LA-MC-ICP-MS are consistent with those obtained by the solution method within ε_{Hf} units (Fig. 7). This is a suitable level of accuracy and precision for usage in tracer studies. However, for ferrotapiolite (713-79), the data obtained by LA-MC-ICP-MS are not accurate or useful due to its high Ta contents.

Matrix effects are well known in LA-MC-ICP-MS analysis. The matrix of CGMs is significantly different, normally with various $Ta^{\#}$ and $Mn^{\#}$. The samples of CGMs in this study are only plotted within ferrocolumbite and manganocolumbite fields (Fig. 2). No matrix effects are observed with the wide range of $Mn^{\#}$. Considering the uncorrected Hf isotopic results of the ferrotapiolite sample (713-79) by LA-MC-ICP-MS caused by the high Ta contents, the validity of our laser analysis method for high $Ta^{\#}$ CGMs (the ferrotantalite and manganotantalite subgroup minerals) needs to be further verified. In natural rare-metal granite- and granitic pegmatite-type Nb–Ta deposits, the ferrotantalite and manganotantalite subgroup minerals normally coexist with ferrocolumbite or manganocolumbite subgroup minerals.[20,21,43,47] The mineral paragenesis indicates the consistency of their source properties in the same magma system. The source properties for this class of ferrotantalite and manganotantalite subgroup minerals could be constrained by analyzing the Hf isotopes of the coexisting ferrocolumbite or manganocolumbite subgroup minerals. Thus, our method should be useful for most Nb–Ta deposits.

Among the natural samples investigated in this study, the CGM sample NP-2 has homogeneous and consistent Hf isotopic components obtained by solution and laser methods, and it also agrees with the Hf isotope of zircon. Moreover, the Yb/Hf and Lu/Hf ratios are relatively low. Thus, sample NP-2 can be used as a potential reference material in the future. In addition, sample Coltan139 has the potential to be a monitor reference material for CGM samples with high Yb/Hf and Lu/Hf ratios because of its homogeneous and consistent Hf isotopic components.

4.3 Advantages and disadvantages of our method

Zircons from rare-metal granites and pegmatites generally have high Yb/Hf ratios. It is difficult to make robust interference corrections during *in situ* Hf isotope analysis of zircons with high Yb/Hf ratios. Most CGMs from rare-metal granites and pegmatites contain 50–2650 ppm Hf and low Yb (Yb/Hf < 0.1) and Lu (Lu/Hf < 0.1) contents (Fig. 8); therefore, CGMs can be used for Lu–Hf isotope analysis. The presented methods for Lu–Hf isotope analysis of CGMs allow this isotopic system to be used as an isotopic tracer for rare-metal deposits. To-date, only Marko *et al.*[38] have briefly mentioned Lu–Hf isotope analysis of CGMs. The solution method described in the present study requires a two-stage chemical separation process. Lutetium can be purified by the Ln Spec resin column, and Hf can be effectively separated from Ta using the AG 1-X8 resin column. This allows accurate and precise Lu–Hf isotope analysis of CGMs and

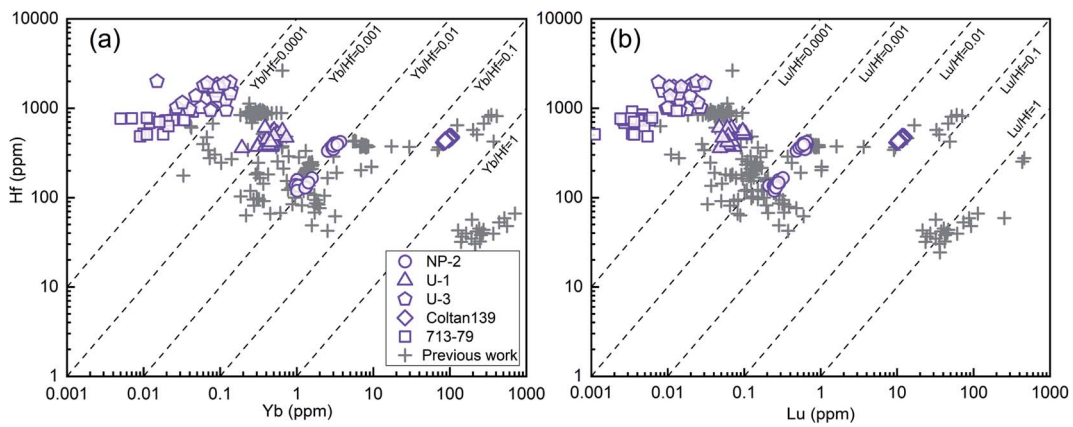

Fig. 8 Plot of Yb *versus* Hf contents (a) and Lu *versus* Hf contents (b) of the CGM and ferrotapiolite samples. Data quoted from Küster *et al.* (2009),[35] Deng *et al.* (2013),[24] Badanina *et al.* (2015),[36] Che *et al.* (2015),[32] Melcher *et al.* (2015),[26] and Feng *et al.* (2020),[37] except the data of samples NP-2, U-1 and U-3 (this study). Only 713-79 is a ferrotapiolite sample; others are CGM samples.

ferrotapiolite by MC-ICP-MS. Better precision can be achieved using the solution method. However, this method has the disadvantages of being time-consuming owing to sample dissolution, and also does not readily allow the determination of spatial variations in the Hf isotopic compositions of CGMs and ferrotapiolite. By normalization to $^{178}Hf/^{177}Hf = 1.4672$, reliable Hf isotopic data for CGMs can be obtained using LA-MC-ICP-MS. This procedure is rapid and relatively inexpensive and allows *in situ* analysis. However, the mineral grain size required is relatively large because of the large laser spot and laser frequency that are necessary. In addition, the significant tailing of Ta affect ^{179}Hf and even ^{178}Hf during *in situ* measurements. It is difficult to obtain precise and accurate $^{176}Hf/^{177}Hf$ data for ferrotapiolite through *in situ* analysis because of its very high Ta content. Therefore, it requires more care during Lu–Hf isotope measurements by LA-MC-ICP-MS than other Ta-rich minerals, such as rutile (*e.g.*, 0.5–40.1 wt% Ta_2O_5;[67] 0.1–14 wt% Ta_2O_5 (ref. 68)) and cassiterite (*e.g.*, 0.09–5.49 wt% Ta_2O_5;[69] 1.1–3.2 wt% Ta_2O_5 (ref. 17)).

CGMs and ferrotapiolite (also called "blood" or "conflict" minerals) have been sold by illegal militias to fund fighting in the Congolese civil war. In order to restrict illegally traded coltan ores, a project to fingerprint Ta–Nb mineral concentrates that was recommended by the United Nations Security Council developed an effective system to identify the origins of CGMs and ferrotapiolite by mineralogical, geochemical, and U–Pb dating methods.[23,26,46,70,71] Each Nb–Ta mineralization system may have a unique Hf isotopic fingerprint (*e.g.*, Fig. 6), which could also be used to identify the sources of Ta–Nb-bearing mineral concentrates in the near future.

5 Conclusions

We have established an improved chemical separation procedure and *in situ* analytical protocol for Lu–Hf isotope analysis of CGMs using MC-ICP-MS. Our conclusions are as follows.

(1) The solution method allows Lu and Hf to be separated from CGMs and ferrotapiolite in a two-column procedure, and results in precise and accurate determination of Lu–Hf concentrations and Hf isotopic compositions by MC-ICP-MS.

(2) *In situ* measurements of Lu–Hf isotopes are feasible by LA-MC-ICP-MS for CGMs, but are difficult for ferrotapiolite. The instrumental mass bias for Hf was corrected to $^{178}Hf/^{177}Hf = 1.4672$ rather than $^{179}Hf/^{177}Hf = 0.7325$, using the exponential law.

(3) Strong peak tailing of Ta may interfere with the ^{179}Hf and even ^{178}Hf signals during (LA)-MC-ICP-MS analysis, which suggests that the effects of Ta on Lu–Hf isotope analysis should also be considered for other Ta-rich minerals.

Conflicts of interest

There are no conflicts of interest to declare.

Acknowledgements

Ru-Cheng Wang acquired the CGM samples (U-1 and U-3) from Prof. Francois Fontan. Unfortunately, we couldn't get the exact information about the samples from Prof. Francois Fontan as we lost him forever. This contribution is dedicated to the late Prof. Francois Fontan in recognition of his great contributions to pegmatology. We would like to thank Yang Li, Xiao-Jun Wang, Zhao-Yu Yang, Ming Yang and Qian Ma for experimental assistance. We are grateful to Yong Tang for his helpful sample collection. This work also benefits from discussions with Jian-Feng Gao, Liang Li and Tao Yang. We thank two anonymous reviewers for their insightful and helpful comments to improve the manuscript. This study was financially supported by the Natural Science Foundation of China (Grants 91855209, 41525012, 41672065 and 41902037) and the Key Research Program of the Institute of Geology & Geophysics, CAS (Grant No. IGGCAS-201902).

References

1 P. J. Patchett, *Geochim. Cosmochim. Acta*, 1983, **47**, 81–91.
2 J. Blichert-Toft, *Geostand. Newsl.*, 2001, **25**, 41–56.
3 F. Y. Wu, Y. H. Yang, L. W. Xie, J. H. Yang and P. Xu, *Chem. Geol.*, 2006, **234**, 105–126.
4 M. F. Thirlwall and A. J. Walder, *Chem. Geol.*, 1995, **122**, 241–247.
5 W. L. Griffin, N. J. Pearson, E. Belousova, S. E. Jackson, E. V. Achterbergh, S. Y. O'Reilly and S. R. Shee, *Geochim. Cosmochim. Acta*, 2000, **64**, 133–147.
6 N. Machado and A. Simonetti, in *Laser-Ablation-ICPMS in the Earth Sciences: Principles and Applications*, ed. P. Sylvester, Mineralogical Association of Canada, 2001, vol. 29, ch. 9, pp. 121–146.
7 W. L. Griffin, X. Wang, S. E. Jackson, N. J. Pearson, S. Y. O'Reilly, X. Xu and X. Zhou, *Lithos*, 2002, **61**, 237–269.
8 U. Söderlund, C. E. Isachsen, G. Bylund, L. M. Heaman, J. P. Patchett, J. D. Vervoort and U. B. Andersson, *Contrib. Mineral. Petrol.*, 2005, **150**, 174–194.
9 F. Bodet and U. Schärer, *Geochim. Cosmochim. Acta*, 2000, **64**, 2067–2091.
10 L. W. Xie, Y. B. Zhang, H. H. Zhang, J. F. Sun and F. Y. Wu, *Sci. Bull.*, 2008, **53**, 1565–1573.
11 F. Y. Wu, Y. H. Yang, M. A. W. Marks, Z. C. Liu, Q. Zhou, W. C. Ge, J. S. Yang, Z. F. Zhao, R. H. Mitchell and G. Markl, *Chem. Geol.*, 2010, **273**, 8–34.
12 G. H. Barfod, O. Otero and F. Albarède, *Chem. Geol.*, 2003, **200**, 241–253.
13 L. N. Kogarko, Y. Lahaye and G. P. Brey, *Mineral. Petrol.*, 2010, **98**, 197–208.
14 Y. Li, Y. H. Yang, S. J. Jiao, F. Y. Wu, J. H. Yang, L. W. Xie and C. Huang, *Sci. China: Earth Sci.*, 2015, **58**, 2134–2144.
15 M. Choukroun, S. Y. O'Reilly, W. L. Griffin, N. J. Pearson and J. B. Dawson, *Geology*, 2005, **33**, 45–48.
16 T. A. Ewing, D. Rubatto, S. M. Eggins and J. Hermann, *Chem. Geol.*, 2011, **281**, 72–82.
17 L. A. Kendall-Langley, A. I. S. Kemp, J. L. Grigson and J. Hammerli, *Lithos*, 2020, **352–353**, 105231.
18 P. Černý and T. S. Ercit, in *Lanthanides, Tantalum and Niobium*, ed. P. Möller, P. Černý and F. Saupé, Springer, Berlin, 1989, ch. 2, pp. 27–79.

19 P. Möller, in *Lanthanides, Tantalum and Niobium*, ed. P. Möller, P. Černý and F. Saupé, Springer, Berlin, 1989, pp. 103–144.
20 R. L. Linnen and M. Cuney, *Rare-Element Geochemistry and Mineral Deposits*, ed. R. L. Linnen and I. M. Samson, Geological Association of Canada, GAC Short Course Notes, 2005, vol. 17, pp. 45–67.
21 R. L. Linnen, M. Van Lichtervelde and P. Cerny, *Elements*, 2012, **8**, 275–280.
22 R. C. Wang, F. Fontan, J. S. Xu, X. M. Chen and P. Monchox, *Can. Mineral.*, 1997, **35**, 699–706.
23 T. Graupner, F. Melcher, H. E. Gäbler, M. Sitnikova, H. Brätz and A. Bahr, *Mineral. Mag.*, 2010, **74**, 691–713.
24 X. D. Deng, J. W. Li, X. F. Zhao, Z. C. Hu, H. Hu, D. Selby and Z. S. de Souza, *Chem. Geol.*, 2013, **344**, 1–11.
25 F. F. Huang, R. C. Wang, L. Xie, J. C. Zhu, S. Erdmann, X. D. Che and R. Q. Zhang, *Ore Geol. Rev.*, 2015, **65**, 761–778.
26 F. Melcher, T. Graupner, H. E. Gäbler, M. Sitnikova, F. Henjes-Kunst, T. Oberthür, A. Gerdes and S. Dewaele, *Ore Geol. Rev.*, 2015, **64**, 667–719.
27 Y. Q. Xiong, S. Y. Jiang, C. H. Wen and H. Y. Yu, *Lithos*, 2020, 358–359, 105422.
28 L. T. Aldrich, G. L. Davis, G. R. Tilton and G. W. Wetherill, *J. Geophys. Res.*, 1956, **61**, 215–232.
29 R. L. Romer and B. Lehmann, *Econ. Geol.*, 1995, **90**, 2303–2309.
30 S. R. Smith, G. L. Foster, R. L. Romer, A. G. Tindle, S. P. Kelley, S. R. Noble, M. Horstwood and F. W. Breaks, *Contrib. Mineral. Petrol.*, 2004, **147**, 549–564.
31 S. Dewaele, F. Henjes-Kunst, F. Melcher, M. Sitnikova, R. Burgess, A. Gerdes, M. A. Fernandez, F. D. Clercq, P. Muchez and B. Lehmann, *J. Afr. Earth Sci.*, 2011, **61**, 10–26.
32 X. D. Che, F. Y. Wu, R. C. Wang, A. Gerdes, W. Q. Ji, Z. H. Zhao, J. H. Yang and Z. Y. Zhu, *Ore Geol. Rev.*, 2015, **65**, 979–989.
33 F. Melcher, T. Graupner, H.-E. Gäbler, M. Sitnikova, T. Oberthür, A. Gerdes, E. Badanina and T. Chudy, *Ore Geol. Rev.*, 2017, **89**, 946–987.
34 X. D. Che, R. C. Wang, F. Y. Wu, Z. Y. Zhu, W. L. Zhang, H. Hu, L. Xie, J. J. Lu and D. Zhang, *Ore Geol. Rev.*, 2019, **105**, 71–85.
35 D. Küster, R. L. Romer, D. Tolessa, D. Zerihun, K. Bheemalingeswara, F. Melcher and T. Oberthür, *Miner. Deposita*, 2009, **44**, 723–750.
36 E. V. Badanina, M. A. Sitnikova, V. V. Gordienko, F. Melcher, H. E. Gäbler, J. Lodziak and L. F. Syritso, *Ore Geol. Rev.*, 2015, **64**, 720–735.
37 Y. Feng, T. Liang, R. Linnen, Z. Zhang, Y. Zhou, Z. Zhang and J. Gao, *Lithos*, 2020, 362–363, 105461.
38 L. Marko, A. Gerdes, F. Melcher and M. Van Lichtervelde, *presented in part at the 21st Meeting of the International Mineralogical Association*, 1–5, September, 2014, Johannesburg, South Africa.
39 C. Münker, S. Weyer, E. Scherer and K. Mezger, *Geochem., Geophys., Geosyst.*, 2001, **2**, 2001GC000183.
40 N. C. Chu, R. N. Taylor, V. Chavagnac, R. W. Nesbitt, R. M. Boella, J. A. Milton, C. R. German, G. Bayon and K. Burton, *J. Anal. At. Spectrom.*, 2002, **17**, 1567–1574.
41 M. F. Thirlwall and R. Anczkiewicz, *Int. J. Mass Spectrom.*, 2004, **235**, 59–81.
42 M. Pfeifer, N. S. Lloyd, S. T. M. Peters, F. Wombacher, B. M. Elfers, T. Schulz and C. Münker, *J. Anal. At. Spectrom.*, 2017, **32**, 130–143.
43 C. Rao, R. C. Wang, H. Hu and W. L. Zhang, *Can. Mineral.*, 2009, **47**, 1195–1212.
44 Y. Tang, J. Y. Zhao, H. Zhang, D. W. Cai, Z. H. Lv, Y. L. Liu and X. Zhang, *Ore Geol. Rev.*, 2017, **83**, 300–311.
45 H. Legros, J. Mercadier, J. Villeneuve, R. L. Romer, E. Deloule, M. Van Lichtervelde, S. Dewaele, P. Lach, X. D. Che, R. C. Wang, Z. Y. Zhu, E. Gloaguen and J. Melleton, *Chem. Geol.*, 2019, **512**, 69–84.
46 H. E. Gäbler, F. Melcher, T. Graupner, A. Bahr, M. A. Sitnikova, F. Henjes-Kunst, T. Oberthur, H. Bratz and A. Gerdes, *Geostand. Geoanal. Res.*, 2011, **35**, 431–448.
47 A. C. Zhang, R. C. Wang, H. Hu, H. Zhang, J. C. Zhu and X. M. Chen, *Mineral. Mag.*, 2004, **68**, 739–756.
48 R. C. Wang, X. D. Che, W. L. Zhang, A. C. Zhang and H. Zhang, *Eur. J. Mineral.*, 2009, **21**, 795–809.
49 R. L. Romer and S. A. Smeds, *Precambrian Res.*, 1996, **76**, 15–30.
50 Y. H. Yang, H. F. Zhang, Z. Y. Chu, L. W. Xie and F. Y. Wu, *Int. J. Mass Spectrom.*, 2010, **290**, 120–126.
51 D. Weis, B. Kieffer, D. Hanano, I. N. Silva, J. Barling, W. Pretorius, C. Maerschalk and N. Mattielli, *Geochem., Geophys., Geosyst.*, 2007, **8**, Q06006.
52 O. Nebel, M. L. A. Morel and P. Z. Vroon, *Geostand. Geoanal. Res.*, 2009, **33**, 487–499.
53 A. Fourny, D. Weis and J. S. Scoates, *Geochem., Geophys., Geosyst.*, 2016, **17**, 739–773.
54 H. L. Lei, T. Yang, S. Y. Jiang and W. Pu, *J. Sep. Sci.*, 2019, **42**, 3161–3276.
55 J. D. Woodhead and J. M. Hergt, *Geostand. Geoanal. Res.*, 2005, **29**, 183–195.
56 L. Yuan, X. J. Wei and H. L. Zhang, *J. Nucl. Radiochem.*, 2013, **35**, 61–64.
57 Y. Chen, *J. Chin. Mass Spectrom. Soc.*, 1999, **20**, 73–80.
58 S. F. Boulyga, U. Klötzli and T. Prohaska, *J. Anal. At. Spectrom.*, 2006, **21**, 1427–1430.
59 L. Tang, K. M. Long and X. M. Liu, *J. Isot.*, 2010, **23**, 44–46.
60 S. F. Boulyga and J. S. Becker, *J. Anal. At. Spectrom.*, 2002, **17**, 1202–1206.
61 Q. Ma, M. Yang, H. Zhao, N. J. Evans, Z. Y. Chu, L. W. Xie, C. Huang, Z. D. Zhao and Y. H. Yang, *J. Anal. At. Spectrom.*, 2019, **34**, 1256–1262.
62 J. P. Faris, *Anal. Chem.*, 1960, **32**, 520–522.
63 E. A. Huff, *Anal. Chem.*, 1964, **36**, 1921–1923.
64 Z. Y. Zhu, R. C. Wang, X. D. Che, J. C. Zhu, X. L. Wei and X. Huang, *Ore Geol. Rev.*, 2015, **65**, 749–760.
65 Y. X. Xiang, J. H. Yang, J. Y. Chen and Y. Zhang, *Ore Geol. Rev.*, 2017, **89**, 495–525.
66 J. F. Chen, H. Zhang, J. X. Zhang and H. Y. Ma, *Chin. J. of Nonferrous Met.*, 2018, **28**, 1832–1844.

67 M. René and R. Škoda, *Mineral. Petrol.*, 2011, **103**, 37–48.
68 K. Breiter, Z. Korbelová, Š. Chládek, P. Uher, I. Knesl, P. Rambousek, S. Honig and V. Šešulka, *Eur. J. Mineral.*, 2017, **29**, 727–738.
69 X. L. Huang, R. C. Wang, X. M. Chen, H. Hu and C. S. Liu, *Can. Mineral.*, 2002, **40**, 1047–1068.
70 F. Melcher, T. Graupner, F. Henjes-Kunst, T. Oberthür, M. Sitnikova, E. Gäbler, A. Gerdes, H. Brätz , D. Davis and D. Dewaele, *Ninth Intern. Congr. Appl. Mineral.*, 2008, pp. 615–624.
71 F. Melcher, M. A. Sitnikova, T. Graupner, N. Martin, T. Oberthür, F. Henjes-Kunst, E. Gäbler, A. Gerdes, H. Brätz, D. W. Davis and S. Dewaele, *SGA News*, 2008, **23**, 1–14.
72 Q. Zhou, PhD thesis, University of Chinese Academy of Sciences, 2013.

